Current Applied Physics 20 (2020) 11–17

Contents lists available at ScienceDirect

Current Applied Physics

journal homepage: www.elsevier.com/locate/cap

Electrostatic spraying of membrane electrode for proton exchange membrane fuel cell

Ruiliang Liu[a], Wei Zhou[a,*], Liyang Wan[b], Pengyang Zhang[b], Shuangli Li[a], Yu Gao[a], Dongsheng Xu[a], Congcong Zheng[c], Mingfeng Shang[d]

[a] Department of Mechanical & Electrical Engineering, Xiamen University, Xiamen, 361005, China
[b] Department of Chemistry, Xiamen University, Xiamen, 361005, China
[c] National Engineering Laboratory for Green Chemical Productions of Alcohols-Ethers-Esters, Xiamen University, Xiamen, 361005, China
[d] Shenzhen Nanko Power Technology Co., Ltd, Shenzhen, 518071, China

ARTICLE INFO

Keywords:
Fuel cell
Membrane electrode
Electrostatic spraying
Platinum-carbon catalytic
Polarization curve

ABSTRACT

In order to improve the performance of proton exchange membrane fuel cell (PEMFC), the optimization of electrostatic spraying of membrane electrode was conducted. The influence of the spraying voltage on morphology, elemental composition of catalyst layer, and performance of the PEMFC were investigated. The results show that increasing spraying voltage could reduce agglomeration of the carbon-supported platinum particles, leading to more uniform pore distribution. High voltage did not accelerate oxidation of platinum catalyst. A high electrochemical active surface area of 26.18 m^2/g_{pt} was obtained when the platinum-carbon catalyst layer was deposited in cone jet mode. With further increasing spraying voltage, the total ohmic resistance and catalytic activity were changed slightly, whereas the charge transfer resistance was increased. Using the optimized electrostatic spraying parameters (injection rate = 100 μL min^{-1}, spraying voltage = 8.5 kV, and working distance = 12 mm), a peak power density of 1.408 W cm^{-2} was obtained with an output voltage of 0.451 V.

1. Introduction

The proton exchange membrane fuel cell is an efficient energy conversion device with wide applications due to its outstanding advantages of large energy density, high energy conversion efficiency, low start-up temperature, and low pollution. The electrochemical reaction generally occurs in the catalyst layer of the membrane electrode assembly (MEA). The method of preparation and microstructure of the catalyst layer have a significant influence on the performance and stability of the PEMFC. As is known, the catalyst layer has a porous structure that is formed by the carbon black component loaded with platinum nanoparticles, and is filled with the proton conducting polymer-Nafion ionomer. The catalyst layer should be conducive to the chemical reaction and to the transfer of fuel gas and water, which can improve the performance of the PEMFC [1]. Therefore, optimization of the composition of the catalyst layer, structural design, and process for preparation for fuel cells is attracting increasing attention.

The catalyst layer of the MEA can be deposited on the proton exchange membrane by the catalyst-coated membrane (CCM) method or deposited on the micropore layer of the gas diffusion layer substrate by the catalyst-coated substrate (CCS) method. The advantages of the CCM method include high utility of the catalyst, excellent proton conductivity between the electrode and membrane, and low interface contact impedance [2–5]. To date, various deposition methods like dipping, doctor blade, screen printing, transfer printing, sputtering, and spraying have been developed for preparing CCM-MEAs. Some methods such as dipping, doctor blade [6], and screen printing [7], with relatively simple working principles and low requirements for equipment and technological processes, were widely applied in the early stage. However, it is difficult to achieve uniformity of the catalyst layers by the above-mentioned methods, leading to agglomeration of the catalyst particles.

The transfer printing method is suitable for mass production of MEAs and can circumvent the problem of expansion or contraction caused by directly coating the wet catalyst slurry onto the membrane. Moreover, the transfer printing method can be used to prepare a thin coating and achieve low interface impedance. However, the transfer processes must be carried out at high temperature, and it is difficult to achieve complete transfer from the substrate to the membrane, resulting in low utilization efficiency of the catalyst [8–13]. The sputtering method can be used to obtain an ultra-thin catalyst layer by strictly controlling the proportions of the catalyst, where good

* Corresponding author.
E-mail address: weizhou@xmu.edu.cn (W. Zhou).

https://doi.org/10.1016/j.cap.2019.09.016
Received 11 July 2019; Received in revised form 21 August 2019; Accepted 26 September 2019
Available online 26 September 2019

polarization characteristics and lower interface contact impedance of the PEMFC have been achieved, even when the platinum loading of the cathode was as low as 0.1 mg cm^{-2}. However, the required special equipment and complex preparation process hinder the mass production of the catalyst layer for MEAs. In addition, the durability of the MEA and inevitable oxidative loss of the catalyst during the sputtering process should be considered [14–18].

Spraying methods, including high pressure air spraying, ultrasonic spraying, and electrostatic spraying, work by destabilizing a fluid by applying high energy to separate small volumes of fluid as tiny droplets. For high pressure air spraying, the atomization energy is derived from high-pressure air turbulence [19]. Ultrasonic spraying provides energy for breaking away droplets from the surface of the solution through high-frequency vibration of the nozzle [20–22]. Electrostatic spraying is a method of dispersing particles on the nanometer scale. Compared with other spraying methods, its attractive advantage is that the trajectory of the charged droplets is determined by the parameters of the electrostatic field. Therefore, multiple scales of droplets can be produced by changing the spraying parameters as required. Previous studies also indicated that the CCM-MEAs prepared by electrostatic spraying still have high catalytic activity, even with quite low platinum loadings [1–3,23–28].

Although electrostatic spraying methods have been used in the preparation of MEAs, there are few reports focusing on the influence of the electrostatic spraying parameters on the microstructure and electrochemical properties of the catalyst layers. In this study, an electrostatic spraying device is designed for experimental evaluation of the relationship between the spraying voltage and the working distance based on analysis of the mechanism of electrostatic spraying. The influence of the spraying voltage on the surface morphology of the Pt/C catalyst layer and the electrochemical properties of a fuel cell assembled with the CCM-MEAs are investigated in detail.

2. Experimental

2.1. Catalyst ink and electrostatic spraying process

The catalyst ink for electrostatic spraying was prepared by mixing Pt/C powder (HISPEC3000, 20 wt%, Johnson Matthey, USA) and Nafion ionomer (D520, 5 wt%, DuPont, USA) in isopropanol solution. Pt/C powder (1 mg) was dissolved in 100 μL of isopropanol solution. The mass fraction of Nafion ionomer accounts for about 30% of the total mass of the catalyst layer [9,22,26]. Before spraying, the catalyst suspension was stirred in an ultrasonic bath for 3 h to ensure sufficient dispersion of the catalyst particles. The surface tension of the catalyst suspension was measured by using a surface tensiometer (DCAT11EC, Dataphysics, Germany).

The special electrostatic spraying equipment for preparation of the MEAs is shown in Fig. 1. The special electrostatic spraying equipment is composed of a high-voltage DC power supply, syringe pump, vacuum heating platform, and three-dimensional movement platform. The high-voltage DC power supply (DW-P503-1ACDE, Dongwen, Tianjin, China) produced a wide range of output voltages from 0 to +30 kV, and was used to generate the electrostatic field for the experiment. The syringe pump (SPLB0-E, ShenChen, Baoding, China) can control the catalyst ink precisely on the order of micro-liters. The vacuum heating platform, as a substrate for the proton exchange membrane, can volatilize the isopropanol solution in time to prevent the membrane from absorbing water and expanding. The three-dimensional movement platform was used to adjust the working distance between the spraying needle and the substrate and drive the motion of the needle. The vacuum heating platform was connected to a ground wire and the stainless steel needle (19G, internal diameter: 0.70 mm) was connected to the DC power supply. The vacuum heating platform was heated to 80 °C before the spraying process. The rate of injection of the catalyst ink was set to 100 μL min^{-1}. The electrostatic spraying parameters are listed in Table 1. Photographs were acquired during the electrostatic spraying process by an industrial camera (MV-EM130C, Microvision, Xi'an, China). The surface morphology of the catalyst layers was observed by using a scanning electron microscope (SEM) (JSM-ITA, JEOL, Japan). The elemental composition of the catalyst before and after the spraying process was characterized by X-ray diffraction (XRD) (JSM-ITA, JEOL, Japan).

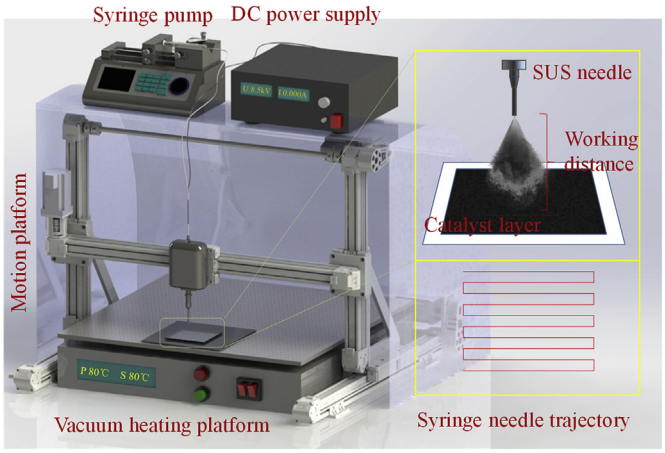

Fig. 1. Schematic diagram of electrostatic spraying.

Table 1
Electrostatic spraying parameters.

Parameters	Value
Dispersing agent	Isopropanol, 99.70 wt%
Catalyst	Pt/C, 20 wt%
Ionomer	Nafion, 5 wt%
Surface tension of catalyst ink	0.024 N m^{-1}
DC voltage	4–15 kV
Working distance	5–15 mm
Substrate temperature	80 °C
XYZ axis motion	60 cm × 100 cm × 100 cm
Injection rate	100 μL min^{-1}
Spraying area	2.25 cm^2

2.2. Fabrication and evaluation of performance of MEAs

The proton exchange membranes (N211, DuPont, USA) coated with the catalyst layers were inserted into two gas diffusion layers (GDLs) to fabricate MEAs with an area of 2.25 cm^2. By controlling the spraying time, the platinum loading in the cathode and anode was set to 0.4 and 0.3 mg cm^{-2}, respectively. The GDL is a hydrophobic carbon paper with a carbon micropore layer on one side (TGP-H-060, TORAT, Japan). In order to reduce the resistance of the MEA, the five-in-one MEA was boned by hot pressing at a pressure of 5 MPa and a constant temperature of 130 °C for 2.5 min. Subsequently, fuel cells with the MEAs and graphite plates of a serpentine flow field were assembled with a uniform force of 7.5 N m.

Fig. 2 shows a schematic diagram of the fuel cell test system. This test system included a mass flowmeter, bubble humidifier, backpressure valve, and electronic load device. The flow rate of the fuel gas and purge gas was controlled by a mass flowmeter (D07-19C, Sevenstar, Beijing, China). The relative humidity of the fuel gas was controlled by adjusting the temperature of the bubble humidifier. The gas pressure of the fuel cell was controlled by backpressure values (Farflow-R51, Panyuan, Shanghai, China). The current–potential (*I–V*) properties were measured by an electronic load device (8513C+, ITECH, Hangzhou, China) at an operating temperature of 80 °C and backpressure of 0.2 MPa. The stoichiometric ratio of H_2 and O_2 was 2; the bubble humidifiers were heated to 80 °C to achieve saturation humidification of

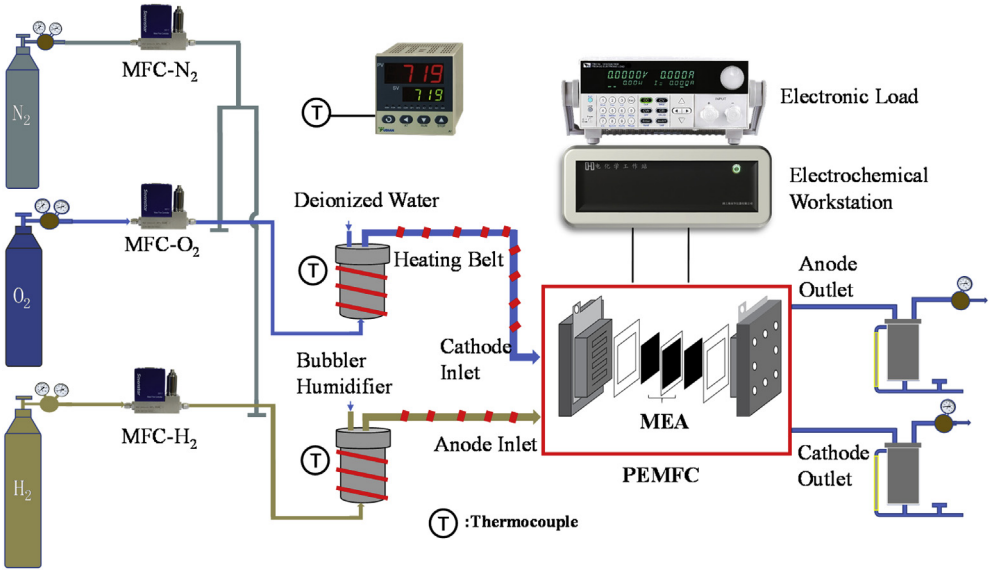

Fig. 2. Schematic diagram of fuel cell test system.

the fuel gas. Before acquisition of the polarization curves, the fuel cells were activated and reached a stable state [29]. Electrochemical impedance spectroscopy (EIS) and cyclic voltammetry (CV) data were acquired by using an electrochemical workstation (Chi660E, ChenHua, Shanghai, China).

During operation of the fuel cell, the anode polarization was negligible relative to the cathode polarization; thus, the anode could be used as the counter-electrode and reference electrode. The EIS measurements were carried out at a cell voltage of 0.5 V with an amplitude of 5 mV, in the frequency range of 0.1 Hz–10 kHz [30]. In order to characterize the catalytic activity and electrochemical active surface area (EASA) of the MEAs prepared by different spraying processes, an electrochemical workstation with a three-electrode setup was used to acquire the CV curves at a scan rate of 50 mV s^{-1} from 0.05 to 1.05 V. The CV measurements were performed at a cell operating temperature of 80 °C with the cathode (humidifying N_2) as the working electrode and anode (humidifying H_2) as the counter-electrode and reference electrode [5,18,30]. The EASA of membrane electrodes can be calculated by applying Eq. (1).

$$EASA = \frac{Q_H}{C \cdot v \cdot M} \quad (1)$$

Where EASA is in m^2 g^{-1}; Q_H is the charge corresponding to the hydrogen oxidation desorption peak in the CV curve (in mC cm^{-2}); v is the scanning speed (in mV s^{-1}); C is the coefficient of hydrogen absorbed on the smooth surface of platinum (0.21 mC cm^{-2}); M is the platinum loading at the cathode (in mg cm^{-2}).

3. Results and discussion

3.1. Analysis of spraying mode

The electrostatic spraying processes for Pt/C catalyst solution with low viscosity has three typical spraying modes, i.e., drip mode (flows in the form of larger droplets), cone jet mode (forms a cone jet at the tip of the needle), and multiple jets mode (forms multiple jets at the tip of needle), as shown in Fig. 3. When the working distance and injection rate are determined, the dropping frequency is accelerated and smaller droplets are produced with increasing spraying voltage. However, the solution cannot be effectively atomized in drip mode. For example, when the droplets make contact with the hot membrane, the isopropanol cannot be evaporated rapidly enough and accumulates on the surface of the membrane. When the spraying voltage is further

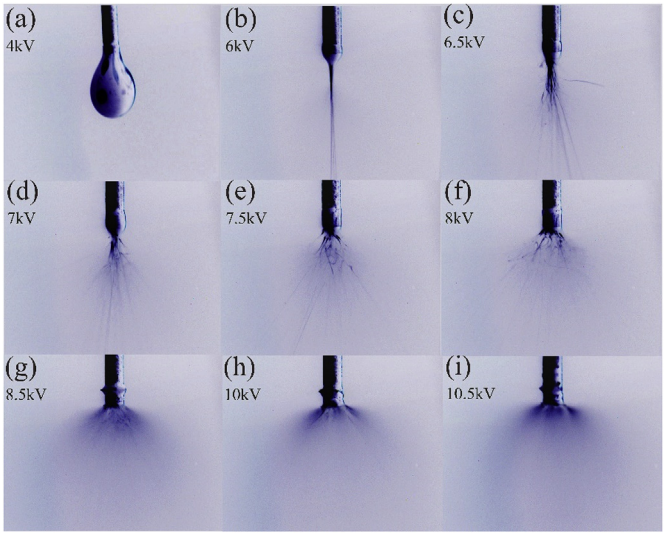

Fig. 3. Typical modes of electrostatic spraying: a) drip mode, b-g) cone jet mode, h-i) multiple jets mode.

increased, the droplet pulse begins to form a stable cone jet and the atomization cone angle also increases gradually. Later, the stable atomization cone jet transforms to unstable multiple jets that rotate along the axis of the jet direction, and the current of the DC power supply increases sharply in this stage. After this stage, increasing the voltage will lead to the breakdown of the electrostatic field.

In order to obtain reasonable electrostatic spraying parameters for preparation of the catalyst layer, the onset voltage for the cone jet mode and the breakdown voltage at different working distances were measured; the catalyst suspension was injected at a rate of 100 μL min^{-1}, as shown in Fig. 4. When the working distance was increased, a larger onset voltage was required to maintain the cone jet. For example, when the working distance was increased from 8 mm to 12 mm, the required onset voltage for maintaining stable cone jet mode increased from 5 kV to 6.2 kV. Meanwhile, the breakdown voltage of the electrostatic field also increased from 8.2 kV to 11.5 kV. Decreasing the working distance and increasing the spraying voltage had a similar influence on atomization of the catalyst solution. This is because atomization of the catalyst solution is determined by the electric field force. Decreasing the working distance and increasing the spraying voltage can enhance the

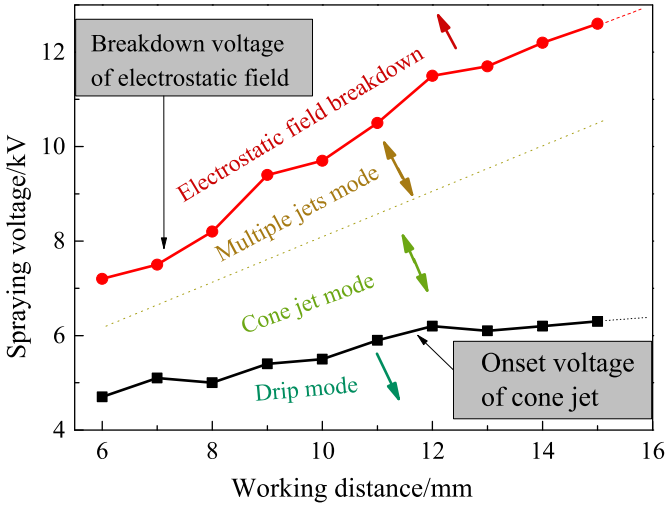

Fig. 4. Electrostatic spraying modes under different parameters.

intensity of the spatial electric field and increase the Coulomb force; therefore, it is easier for the droplets of the catalyst solution to break away from the surface of the suspension and split into tiny particles.

In addition, the onset voltage of the cone jet mode can be predicted by Smith's formula (2) [28,31]. Where, r_c is the inner diameter of the stainless steel needle (0.70 mm) and γ is the surface tension of the suspension. In this study, the surface tension of the catalyst suspension was 0.025 N m^{-1}; θ_0 is the half-angle of the cone-jet, where Taylor used a value of 49.3° [28]; L is the working distance; ε is the dielectric constant: 8.85 × 10^{-12} F m^{-1}.

$$V_0 = A\left(\frac{2r_c\gamma\cos\theta_0}{\varepsilon}\right)^{\frac{1}{2}} ln\left(\frac{4L}{r_c}\right) \quad (2)$$

Notably, A is an empirical constant defined by Smith [31]. In this study, the Smith constant A was determined to be 0.79 by parameter fitting of the experimental results. The results predicted by Smith's formula are shown in Table 2. The theoretical results were consistent with the present experimental results. Therefore, Smith's formula (A = 0.79) can be used to predict the onset voltage of the cone jet mode.

3.2. Effect of spraying voltage on surface morphology of catalyst layer

Fig. 5 shows the SEM image of the catalyst layers prepared with different spraying voltages. The injection rate of the suspension was 100 μL min^{-1} and the working distance was 12 mm. The catalyst layer prepared in cone jet mode with 6.5 kV spraying voltage exhibited high porosity, as shown in Fig. 5a. Agglomerated Pt/C particles were distributed in the catalyst layer and spherical carbon particles were relatively uniformly dispersed on the sub-micron scale (100 nm − 1 μm). Increasing the spraying voltage could reduce agglomeration of the carbon-supported platinum particles. A more uniform pore distribution in the catalyst layer was obtained with a spraying voltage of 8.5 kV, as shown in Fig. 5b. When the spraying voltage was increased to 10.5 kV and the spraying mode of the cone jet was changed to multiple jets, much more uniform distribution of the catalyst particles was observed (Fig. 5c). However, obvious agglomeration of the catalyst particles was also found in the catalyst layer prepared in multiple jets mode.

The surface morphology of the catalyst layer prepared by electrostatic spraying is determined by the composition of the catalyst solution and spraying process parameters [1]. With higher spraying voltage, higher electricity per unit mass of the catalyst solution and coulomb repulsive force were obtained, which led to a larger umbrella cone angle. Therefore, a high spraying voltage is beneficial for preventing agglomeration of the droplets to prepare highly dispersed particles. However, an unstable atomization process even the breakdown of electrostatic field occurs in multi-jet mode, and the size of the droplets does not decrease with increasing spraying voltage. Thus, the non-homogeneous size of the Pt/C particles was obtained.

3.3. Effect of spraying voltage on composition of catalyst

The catalyst composition before and after the electrostatic spraying process at a high voltage of 10.5 kV was analyzed by X-ray diffraction (XRD). Fig. 6 shows the XRD spectra of the Pt/C catalyst before and after the spraying process. Before the spraying process, two peaks of crystalline species were observed at 2θ = 39° and 46°, corresponding to the (111) and (200) planes of face cubic centered (fcc) polycrystalline Pt. The intensity of the peak corresponding to the Pt (111) plane was much higher than that of the Pt (200) plane, which indicated that the (111) direction is the predominant growth direction of the Pt crystal. The XRD spectra also show two diffraction peaks at 2θ = 25° and 18° for carbon and the Nafion ionomer. Comparison of the XRD spectra before and after the spraying process shows that the peak of Nafion in the MEA after the spraying process was much more intense than that before the spraying process. This difference can be attributed to the higher content of Nafion in the CCM-MEA than that in the catalyst suspension because the catalyst layer is deposited on the Nafion membrane. Furthermore, no diffraction peak of platinum oxide was observed in the XRD spectra, which indicated that platinum oxide was not produced during the spraying process. Thus, oxidative loss of the precious metal platinum can be ignored.

3.4. Electrochemical properties of MEAs

The MEAs were prepared by employing three different spraying voltages (6.5, 8.5, and 10.5 kV). The polarization curves and power density curves of the fuel cells assembled with the MEAs are shown in Fig. 7. In the electrochemical polarization region spanning the current density range of 0–0.5 A cm^{-2}, the potential decreased rapidly due to activation loss caused by the reaction kinetics. The performance of the MEAs prepared at 6.5 and 8.5 kV was much better than that prepared at 10.5 kV. When the fuel cell was operated in the ohmic polarization region, the potential decreased linearly within a wide current range. The peak power density of the MEAs prepared at 6.5 and 10.5 kV was 1.19 and 0.751 W cm^{-2}, respectively. The MEA prepared at 8.5 kV exhibited the best performance with a peak power density of 1.408 W cm^{-2} at a potential of 0.451 V. However, the MEA prepared at 10.5 kV showed much poorer performance in each polarization region, and concentration polarization occurred earlier, thus limiting the reaction.

Fig. 8 shows the CV curves of the different MEAs. The EASA was calculated from the charge of hydrogen desorption in the potential range of 0.12–0.4 V [18,30], as shown in Fig. 9. The EASA of the MEAs

Table 2
Onset voltages comparison between experimental results and Smith's formula.

Working distance (mm)		6.0	7.0	8.0	9.0	10.0	11.0	12.0	13.0	14.0	15.0
Onset voltage (kV)	Experiment	4.70	5.10	5.00	5.40	5.50	5.90	6.20	6.10	6.20	6.30
	Smith's	4.90	5.11	5.29	5.46	5.60	5.73	5.85	5.96	6.06	6.16
	Error value	0.20	0.01	0.29	0.06	0.10	0.17	0.35	0.14	0.14	0.14

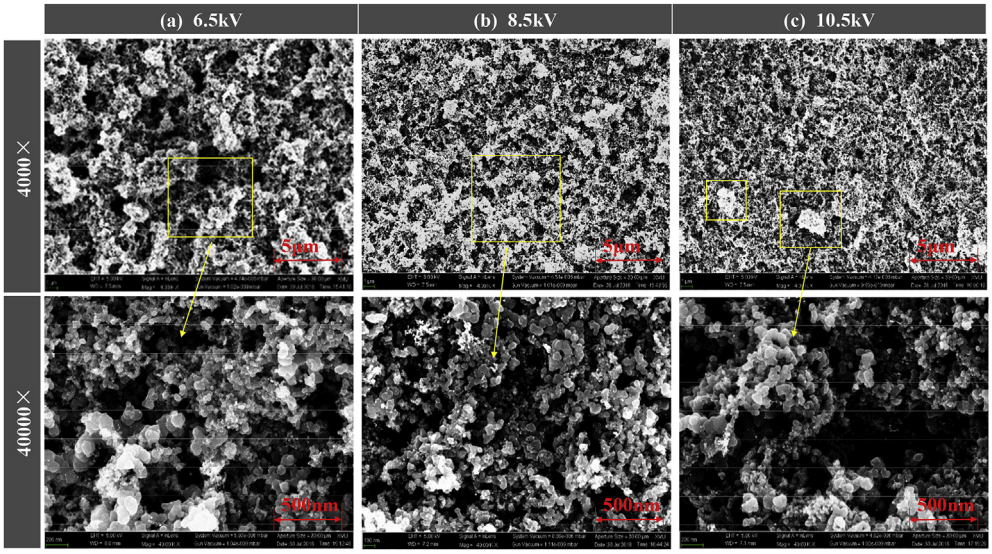

Fig. 5. Surface morphology of catalyst layers prepared with different spraying voltages. a) 6.5 kV, the initial stage of cone jet formation; b) 8.5 kV, the transition stage from cone-jet to multiple jet; c) 10.5 kV, the critical stage of electrostatic field breakdown.

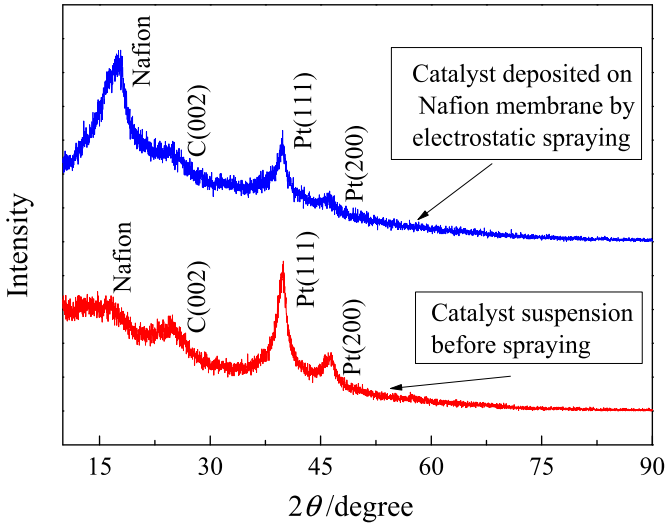

Fig. 6. XRD spectra of Pt/C catalyst before and after spraying process.

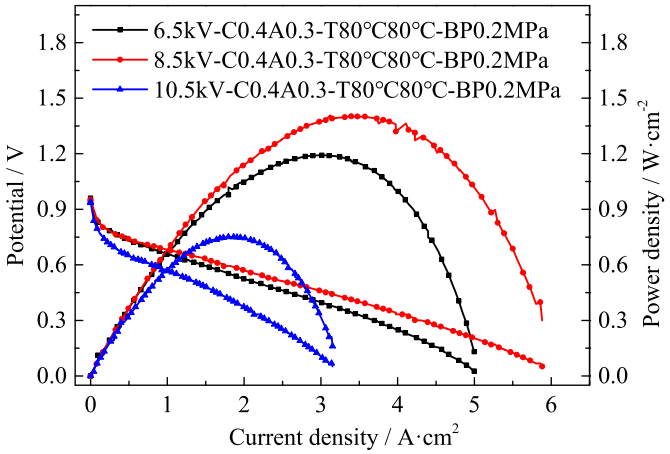

Fig. 7. Polarization and power density curves of fuel cells assembled with the MEAs.

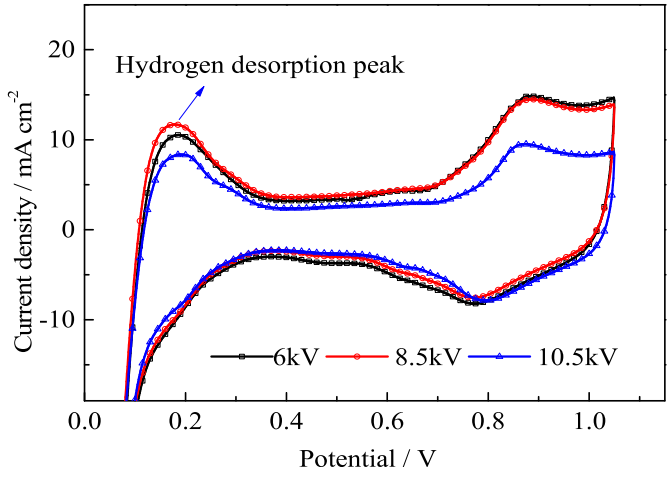

Fig. 8. CV curves of different MEAs.

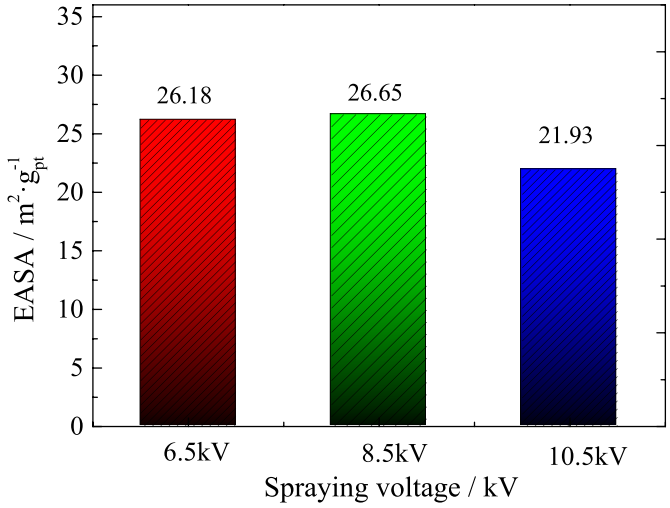

Fig. 9. EASA of membrane electrodes prepared under different spraying voltages.

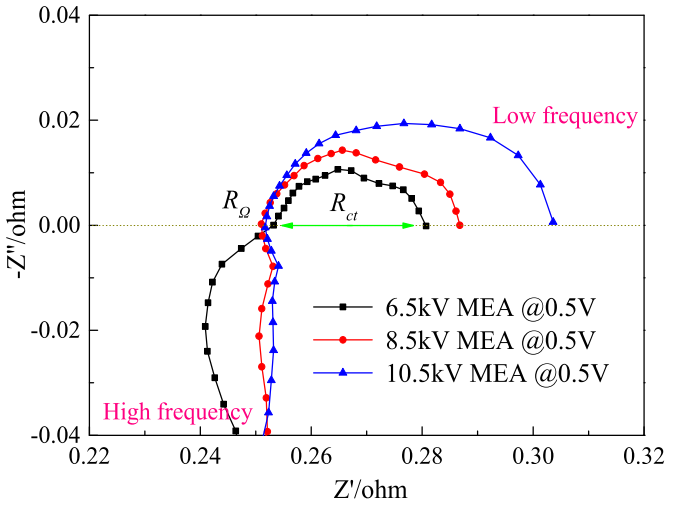

Fig. 10. Nyquist curves of different fuel cells under operating voltage of 0.5 V

prepared at the three spraying voltages of 6.5, 8.5, and 10.5 kV were 26.18, 26.65, and 21.93 m^2/g_{Pt}, respectively. These results indicate that the catalyst layers prepared at spraying voltages of 6.5 and 8.5 kV possessed a large catalytically active area. Although higher spraying voltage could improve the dispersion of the catalyst particles, the catalytic active area did not increase significantly when the spraying voltage was increased to 8.5 kV. On the contrary, low catalytic activity was obtained with the MEAs prepared at a critical breakdown voltage of 10.5 kV.

The EASA results are consistent with the trends of the polarization curves. This can be attributed to a decrease in the particle size of the catalyst with increasing spraying voltage, which is beneficial for generating a three-phase reaction interface between the Nafion ionomer and platinum particles. In this way, the utilization of the catalysts can be effectively improved. Therefore, the electrochemical performance of the MEA prepared at 8.5 kV was better than that prepared at 6.5 kV. As the spraying voltage further was increased to approximate the breakdown voltage of electrostatic field, the non-homogeneous pore distribution and obvious agglomeration of the catalyst particles was obtained in the catalyst layer prepared in the unstable multiple jets mode, which inevitably hinder the surface of the platinum for reaction and reduce the utilization of the catalyst. Meanwhile, the highly dispersed catalyst particles in the MEA prepared at 10.5 kV made the catalyst layer favorable for retaining water. The retained water blocks the fuel gas flow and reduces the utilization of the catalyst [9,18,32]. Consequently, the MEA prepared at 10.5 kV exhibited relatively poor performance.

The electrochemical impedance of the MEA was further investigated by EIS. The impedance performance of different fuel cells is expressed by the Nyquist curves, as shown in Fig. 10. The approximately semicircular arc in the Nyquist curve indicates that the electrode reaction is mainly controlled by the interface kinetics of the oxidation-reduction reaction [5,30]. The high-frequency intercept on the real axis corresponds to the total ohmic resistance (R_Ω), which is the sum of the ohmic resistance of each cell component and their interfacial contact resistance. As shown in Fig. 10, the ohmic resistances of different fuel cells are approximately equal, which can be attributed to the dominant effect of the DuPont N211 proton exchange membrane on the ohmic resistance of the fuel cell. Meanwhile, it should be noted that the total ohmic resistance of MEA prepared at 6.5 kV was slightly larger than two other MEAs, which could be attributed to the increase of interfacial contact resistance because of the agglomeration of catalyst particles and non-uniform pore distribution in catalyst layer. Under the combined influence of R_Ω and R_{ct}, in the ohmic polarization region, the polarization curve of the MEAs prepared at 6.5 kV exhibits a steeper slope than the 8.5 kV one. The diameter of the semicircular arc in the Nyquist curve represents the charge transfer resistance (R_{ct}) in the oxidation-reduction reaction. With an increase of the spraying voltage from 6.5 to 10.5 kV, the charge transfer resistance of the fuel cell increased from 0.124 to 0.134 Ω. The above results can be attributed to destruction of the proton pathways in the catalyst layer by the high spraying voltage. The absence of continuous Nafion ionomers impeded proton transfer and eventually led to an increase in the charge transfer resistance.

4. Conclusions

An electrostatic spraying device was designed and a single fuel cell test system was established. Three typical electrostatic spraying modes were utilized; the onset voltages of the cone jet mode at different working distances were then determined by experimental evaluation and numerical calculation. The results show that with an increase of the spraying voltage from 6.5 to 8.5 kV, agglomeration of the carbon-supported platinum particles could be reduced, and a more uniform pore distribution in the catalyst layer was obtained. Oxidation of the platinum-carbon catalyst was not accelerated by high spraying voltage. A high electrochemical active surface area of 26.18 m^2/g_{pt} could be obtained when the platinum-carbon catalyst layer was deposited in cone jet mode. The total ohmic resistance and catalytic activity changed slightly with further increasing spraying voltage, whereas the charge transfer resistance increased. Using the electrostatic spraying parameters of 100 μL min^{-1} injection rate, 8.5 kV spraying voltage, and 12 mm working distance, a peak power density of 1.408 W cm^{-2} was obtained with a potential of 0.451 V. This study provides a feasible method for preparation and optimization of the catalyst layer by using electrostatic spraying, which has promising application for the efficient utilization of catalysts and improving the performance of PEMFCs.

Acknowledgments

This work was supported by the Natural Science Foundation of China (No.51922092) and Natural Science Foundation of Fujian Province of China (No. 2017J06015). In addition, the supports from the Fundamental Research Funds for Central Universities, Xiamen University (No. 20720190031 and 20720190129).

References

[1] A.M. Chaparro, M.A. Folgado, P. Ferreira-Aparicio, A.J. Martin, I. Alonso-Alvarez, L. Daza, Properties of catalyst layers for PEMFC electrodes prepared by electrospray deposition, J. Electrochem. Soc. 157 (2010) B993–B999.
[2] A.M. Chaparro, P. Ferreira-Aparicio, M.A. Folgado, A.J. Martín, L. Daza, Catalyst layers for proton exchange membrane fuel cells prepared by electrospray deposition on Nafion membrane, J. Power Sources 196 (2011) 4200–4208.
[3] S. Martin, B. Martinez-Vazquez, P.L. Garcia-Ybarra, J.L. Castillo, Peak utilization of catalyst with ultra-low Pt loaded PEM fuel cell electrodes prepared by the electrospray method, J. Power Sources 229 (2013) 179–184.
[4] J. Zhang, G. Yin, Z. Wang, Y. Shao, Effects of MEA preparation on the performance of a direct methanol fuel cell, J. Power Sources 160 (2006) 1035–1040.
[5] N. Shan, H. Jung, J.Y. Ahn, J.H. Kim, S.H. Kim, Electrospray-assisted fabrication of porous platinum-carbon composite thin layers for enhancing the electrochemical performance of proton-exchange membrane fuel cells, Curr. Appl. Phys. 18 (2018) 728–736.
[6] I.-S. Park, W. Li, A. Manthiram, Fabrication of catalyst-coated membrane-electrode assemblies by doctor blade method and their performance in fuel cells, J. Power Sources 195 (2010) 7078–7082.
[7] W. Wang, S. Chen, J. Li, W. Wang, Fabrication of catalyst coated membrane with screen printing method in a proton exchange membrane fuel cell, Int. J. Hydrogen Energy 40 (2015) 4649–4658.
[8] X. Liang, G. Pan, L. Xu, J. Wang, A modified decal method for preparing the membrane electrode assembly of proton exchange membrane fuel cells, Fuel 139 (2015) 393–400.
[9] S. Mu, M. Tian, Optimization of perfluorosulfonic acid ionomer loadings in catalyst layers of proton exchange membrane fuel cells, Electrochim. Acta 60 (2012) 437–442.
[10] T. Suzuki, S. Tsushima, S. Hirai, Effects of Nafion® ionomer and carbon particles on structure formation in a proton-exchange membrane fuel cell catalyst layer fabricated by the decal-transfer method, Int. J. Hydrogen Energy 36 (2011) 12361–12369.

[11] Y.J. Yoon, T.-H. Kim, S.U. Kim, D.M. Yu, Y.T. Hong, Low temperature decal transfer method for hydrocarbon membrane based membrane electrode assemblies in polymer electrolyte membrane fuel cells, J. Power Sources 196 (2011) 9800–9809.
[12] S. Shahgaldi, I. Alaefour, G. Unsworth, X. Li, Development of a low temperature decal transfer method for the fabrication of proton exchange membrane fuel cells, Int. J. Hydrogen Energy 42 (2017) 11813–11822.
[13] M.S. Saha, D.K. Paul, B.A. Peppley, K. Karan, Fabrication of catalyst-coated membrane by modified decal transfer technique, Electrochem. Commun. 12 (2010) 410–413.
[14] Y.-C. Lai, K.-L. Huang, C.-H. Tsai, W.-J. Lee, Y.-L. Chen, Sputtered Pt loadings of membrane electrode assemblies in proton exchange membrane fuel cells, Int. J. Energy Res. 36 (2012) 918–927.
[15] M.S. Çögenli, S. Mukerjee, A.B. Yurtcan, Membrane electrode assembly with ultra low platinum loading for cathode electrode of PEM fuel cell by using sputter deposition, Fuel Cells 15 (2015) 288–297.
[16] Y.S. Li, T.S. Zhao, Ultra-low catalyst loading cathode electrode for anion-exchange membrane fuel cells, Int. J. Hydrogen Energy 37 (2012) 15334–15338.
[17] Z. Tang, C.K. Poh, K.C. Chin, D.H.C. Chua, J. Lin, A.T.S. Wee, Cobalt coated electrodes for high efficiency PEM fuel cells by plasma sputtering deposition, J. Appl. Electrochem. 39 (2009) 1821–1826.
[18] H. Yu, J.M. Roller, W.E. Mustain, R. Maric, Influence of the ionomer/carbon ratio for low-Pt loading catalyst layer prepared by reactive spray deposition technology, J. Power Sources 283 (2015) 84–94.
[19] B.M. Koraishy, J.P. Meyers, K.L. Wood, Manufacturing of direct methanol fuel cell electrodes by spraying, J. Electrochem. Soc. 158 (2011) B1459–B1471.
[20] B. Millington, V. Whipple, B.G. Pollet, A novel method for preparing proton exchange membrane fuel cell electrodes by the ultrasonic-spray technique, J. Power Sources 196 (2011) 8500–8508.
[21] J.H. Bang, K. Han, S.E. Skrabalak, H. Kim, K.S. Suslick, Porous carbon supports prepared by ultrasonic spray pyrolysis for direct methanol fuel cell electrodes, J. Phys. Chem. C 111 (2007) 10959–10964.
[22] T.-H. Huang, H.-L. Shen, T.-C. Jao, F.-B. Weng, A. Su, Ultra-low Pt loading for proton exchange membrane fuel cells by catalyst coating technique with ultrasonic spray coating machine, Int. J. Hydrogen Energy 37 (2012) 13872–13879.
[23] R. Benítez, J. Soler, L. Daza, Novel method for preparation of PEMFC electrodes by the electrospray technique, J. Power Sources 151 (2005) 108–113.
[24] M. Umeda, S. Kawaguchi, I. Uchida, Characterization of membrane electrode assembly for fuel cells prepared by electrostatic spray deposition, Jpn. J. Appl. Phys. 45 (2006) 6049–6054.
[25] A.M. Chaparro, R. Benítez, L. Gubler, G.G. Scherer, L. Daza, Study of membrane electrode assemblies for PEMFC, with cathodes prepared by the electrospray method, J. Power Sources 169 (2007) 77–84.
[26] A.M. Chaparro, B. Gallardo, M.A. Folgado, A.J. Martín, L. Daza, PEMFC electrode preparation by electrospray: optimization of catalyst load and ionomer content, Catal. Today 143 (2009) 237–241.
[27] S. Martin, P.L. Garcia-Ybarra, J.L. Castillo, Electrospray deposition of catalyst layers with ultra-low Pt loadings for PEM fuel cells cathodes, J. Power Sources 195 (2010) 2443–2449.
[28] N. Chingthamai, K. Sombatmankhong, Y. Laoonual, Experimental investigation of electrospray coating technique for electrode fabrication in PEMFCs, Energy Procedia 105 (2017) 1806–1812.
[29] D.K. Shin, J.H. Yoo, D.G. Kang, M.S. Kim, Effect of cell size in metal foam inserted to the air channel of polymer electrolyte membrane fuel cell for high performance, Renew. Energy 115 (2018) 663–675.
[30] H. Su, T.-C. Jao, O. Barron, B.G. Pollet, S. Pasupathi, Low platinum loading for high temperature proton exchange membrane fuel cell developed by ultrasonic spray coating technique, J. Power Sources 267 (2014) 155–159.
[31] P.H.D. Smith, The electrohydrodynamic atomization of liquids, IEEE Trans. Ind. Appl. IA-22 (1986) 527–535.
[32] B.-S. Koh, J.-H. Yoo, E.-K. Jang, V.R. Jothi, C.-Y. Jung, S.C. Yi, Fabrication of highly effective self-humidifying membrane electrode assembly for proton exchange membrane fuel cells via electrostatic spray deposition, Electrochem. Commun. 93 (2018) 76–80.